IEEE Access
Multidisciplinary | Rapid Review | Open Access Journal

Received May 31, 2018, accepted July 22, 2018, date of publication August 7, 2018, date of current version September 21, 2018.

Digital Object Identifier 10.1109/ACCESS.2018.2864102

Study on the Scattering Effect of Terahertz Waves in Near-Surface Atmosphere

QINGFENG JING[1], DANMEI LIU[1], AND JINCHENG TONG[2]
[1]College of Astronautics, Nanjing University of Aeronautics and Astronautics, Nanjing 210019, China
[2]Institute of Telecommunication Satellite, China Academy of Space Technology, Beijing 100000, China

Corresponding author: Qingfeng Jing (jing_nuaa@163.com)

This work was supported by the Fundamental Research Funds for the Central Universities under Grant NS2017069.

ABSTRACT Terahertz waves suffer from scattering attenuation of various types of particles due to the complex environment in the near-surface atmosphere. This paper focused on the scattering attenuation of terahertz waves due to different kinds of particles, including droplets, haze particles, and raindrops. The optical parameters of these particles were determined by meteorological data and the related literature. The characteristics of the scattering attenuation of terahertz waves on hazy days were analyzed using Rayleigh scattering and the lognormal distribution of particles, based on different levels of pollution and frequency. The basic physical characteristics of fog were also examined to determine the influence of water content on the visibility and size distribution of droplets. The scattering characteristics of terahertz waves caused by advection fog and radiation fog were assessed using the Mie scattering theory based on the complex index of droplet refraction. Then, the characteristics of scattering attenuation in fog days were identified under different levels of visibility. The Rayleigh approximation method was used to numerically model the scattering effect of small droplets and the effect of temperature and visibility on characteristic attenuation. Results show that, by comparing the distribution of different raindrop sizes, the Joss distribution was found to be quite accurate. Raindrop size distribution and scattering attenuation characteristics under different rainfall rates were identified using the Mie scattering method. The meteorological environment is complex in the near-earth atmosphere and the scattering attenuation of terahertz waves under fog, hazy, and rainy conditions cannot be ignored. Meteorological factors, such as visibility and rainfall rate, exert critical influences on the scattering attenuation characteristics of terahertz waves.

INDEX TERMS Terahertz, scattering attenuation, Mie theory, Rayleigh theory, channel modeling.

I. INTRODUCTION

Terahertz wireless communication technology provides a new solution for ultra-high-speed wireless communication given a shortage of frequency-band resources. The channel model of terahertz bands is indispensable to the design of physical-layer technology and accurate performance analysis for the terahertz communication system. The study of attenuation characteristics of terahertz waves transmitted in the near-surface atmosphere is therefore important. Existing channel models include free-space path loss and molecular absorption attenuation [1]. However, few systematic research has been conducted on the scattering loss of different particles suspended in the atmosphere, which is essential for establishing a complete terahertz communication channel model. The ability of terahertz waves to penetrate the atmosphere is weak. Waves are easily scattered by particles such as droplets and raindrops in the atmosphere, causing attenuation of the terahertz signal [2]. Haze pollution becomes more and more serious in China in recent years, which lead to serious attenuation of the transmission of terahertz waves. Complex weather phenomena reduce the intensity of signals reaching the receiving equipment, compromising the detection ability of terahertz waves and influencing the performance of terahertz communications systems substantially. As such, a study of the transmission characteristics of terahertz waves in complex atmospheric environments is essential.

Scattering loss [3] is an important source of attenuation of terahertz waves when propagating in the atmosphere. Suspended particles in the atmosphere exhibit a certain degree of stability with a small settling velocity, including rain, fog, haze, clouds, dust, carbon particles, salt crystals, and tiny living organisms with scales in the range of $10^{-3}\mu$m–100μm.

Aerosols in the near-earth atmosphere include raindrops, droplets, and haze particles. Different particles obey different scale distributions; haze particles range from 0.01μm to several micrometers, fog particles are generally within 1μm–100μm, and the radius of raindrops generally range from 0.05mm–4mm. Table 1 lists the scale range and number density of various particles in the near-surface atmosphere.

As early as 1976, Ishimaru and Hong [4] numerically studied the transmission characteristics of 0.649-μm and 10.6-μm light pulses under conditions of rain, fog, and turbulence. In 1978, Dougherty and Dutton [5] proposed a segmented atmospheric transmission model for frequency bands up to 0.35 THz, accounting for attenuation and phase-delay characteristics under different weather conditions such as a clear sky, clouds, and rainfall. Liebe [6] proposed an atmospheric millimeter wave propagation model in 1989. The model was later modified and improved several times. The model is physical and includes the effects of dry air, suspended water droplets, and rain; it is mainly used to calculate loss and delay effects in the neutral atmosphere. Vasseur and Gibbins [7] conducted experiments on 10.6-μm infrared light and 0.63-μm visible light in rain in 1996. Data revealed signal loss of the 10.6-μm light to be approximately 50% higher than that of the 0.63-μm light. Lakshmi *et al.* [8] studied raindrop scale distribution and the attenuation of frequency bands ranging from11GHz to12.25GHzfor wireless communication in 2007. Raindrops ranging in size between 0.771mm–5.3mm exerted a severe impact on scale distribution and attenuation. David *et al.* [9] studied the attenuation of near-infrared and far-infrared waves in an artificial fog environment and found that the attenuation of near-infrared waves was much greater than that of far-infrared waves. Kokkoniemi and Lehtomäki [10] studied the scattering attenuation of terahertz waves using atmospheric aerosol particles and a calculation method involving a scattering cross-section of atmospheric molecules. Scholars from different countries have conducted extensive research on the scattering effects of terahertz waves caused by atmospheric aerosols [11], [12]. For instance, Akyildiz and Jornet [13] studied the scattering nature of terahertz waves using aerosol particles and discovered that Rayleigh scattering dominates.

Many research institutes in China also study the propagation characteristics of the atmosphere and hydrometeors. Zhao and Wu [14] of the China Institute of Radio Wave Propagation examined the attenuation, scintillation, and radar backscattering characteristics of 3-mm waves in sea fog and established an empirical formula for the attenuation of electromagnetic waves in a cloud at wavebands of 10–1,000 GHz. The team of academician Yao Jianxi at Tianjin University [15] studied the transmission characteristics of THz waves. Zhang Min [16] at Xidian University used the finite difference-time domain method to study the propagation characteristics of THz waves.

Studies have revealed that the essence of scattering involves the physical process of energy redistribution. The spatial distribution of scattered light radiation is not uniform; the effect of atmospheric scattering on terahertz waves is mainly reflected in the attenuation of light intensity and the variation in light intensity distribution in the propagation direction. The scattering law in the atmosphere varies with the size of scattering particles. As the terahertz wavelength range is generally between 300μm–3mm, many suspended particles in the air satisfy scattering conditions. The scattering process of single particles on a terahertz wave is independent, generally calculated based on the principles of Rayleigh scattering and Mie scattering. Table 1 presents attenuation calculation models applicable to various matters.

TABLE 1. Particle parameters and attenuation simulation model of different substances.

Particle type	Radius/μm	Number density($1/cm^{-3}$)	Attenuation model
Molecular	10^{-4}	10^{19}	Line-by-line integration
Aitkennuclei	10^{-3}~10^{-2}	10^{2}~10^{4}	Rayleigh scattering
Haze particle	10^{-2}~1	10~10^{3}	Rayleigh scattering
Fog droplet	1~10	10~100	Mie scattering
Rain drop	10^{2}~10^{4}	10^{-2}~10^{-5}	Mie scattering

Based on electromagnetic scattering theory, this paper combines meteorological data and relevant literature to determine the particle complex refractive index and optical characteristic parameters (e.g., scale distribution of rain, fog, and haze). The extinction parameters of atmospheric aerosols at different scales and the characteristic attenuation of terahertz waves are calculated. Section 2 analyzes the physical parameters of the atmospheric environment, particle scattering, and influencing factors. Section 3 briefly introduces the existing classical particle scattering theory, identified particle characteristics and scattering analysis theory to perform numerical calculations.

II. ANALYSIS OF PHYSICAL PARAMETERS OF ATMOSPHERIC ENVIRONMENT, SCATTERING PARTICLES, AND INFLUENCING FACTORS

A. PHYSICAL CHARACTERISTICS OF HAZE

Aerosols in the troposphere have different origins and different shapes along with wide-scale distributions, with clusters as small as a radius of 100 pm. Particles with a radius of less than 0.1μm are often referred to as Aitken nuclei, those measuring0.1–1μm are large particles, and particles larger than 1μm are giant particles; all are considered haze. Haze is the most common natural phenomenon in the atmosphere, composed primarily of extremely fine dust, small salt crystal grains, and some burnt products consisting of fine particles dispersed in the air. Weather maps from the China Meteorological Administration provide statistical data on the density of haze and fog particles (Table 2).

When haze occurs, the air contains hundreds of atmospheric particles. Aerosol particles with a diameter of less

TABLE 2. Particle number density statistics of haze.

Diameter	Minimum	25%	Median	75%	Maximum	Average	Standard deviation
0.3~0.5μm	25	107	170	246	346	176	82
0.5~0.7μm	2	9	17	33	152	24	21
0.7~1.0μm	0.4	2	3	7	46	5	5
1.0~2.0μm	0.2	~	3	5	65	4	4
2.0~5.0μm	0.1	1	1	2	61	2	3
>5.0μm	0	0	0	0.1	11	0.1	0.5
Total number density	28	123	197	294	510	211	107

than 10μmpostthe most serious health hazards. Due to a large amount of dust, microorganisms, and particulates, the cleanliness and visibility of haze are extremely low. The composition of haze is highly complicated. Most studies have been based on PM2.5 and PM10 mass concentration to describe haze particle distribution and characteristics.

According to the China Environmental Bulletin of 2017, an analysis of various indicators showed that the PM2.5 concentration throughout 2017 ranged from 12–158$\mu g/m^3$ with an average value of 47$\mu g/m^3$; PM10 concentrations ranged from 22–436$\mu g/m^3$ with an average value of82 $\mu g/m^3$, and O_3 concentration in a maximum 8-hour window ranged from 73–200$\mu g/m^3$ with an average value of 138 $\mu g/m^3$. SO_2 concentration ranged from 3–88$\mu g/m^3$ with an average value of 22$\mu g/m^3$, NO_2 concentration ranged from 9–61$\mu g/m^3$ with an average value of 30$\mu g/m^3$, and CO concentration ranged from 0.8–5.0mg/m^3 with an average value of 1.9mg/m^3. The size of aerosol scattering particles can vary, but particle density distribution usually obeys a lognormal distribution [17]; thus, a lognormal distribution is applied to aerosol particles, defined as [18], [19]:

$$\mathrm{N(D)} = \frac{dN}{dD} = \frac{1}{D\sqrt{2\pi}\ln(\sigma_g)} e^{-\frac{(\ln(D)-\ln(r_g))^2}{2\ln(\sigma_g)^2}} \quad (1)$$

Where r_g is the average geometric diameter of the scattered particles, D is their diameter, σ_g is the corresponding standard deviation, and N_s is the number of haze particles per unit volume. The number density distribution of particles in hazy weather can be obtained based on observations of the haze process. Pollutant distribution parameters across different levels are presented in Table 3.

Eq.(1) is multiplied by the number density to obtain the particle spectrum distribution. Haze particle distribution at different levels of pollution is shown in Fig. 1.

Only larger haze particles have a strong scattering effect on terahertz wave. According to scattering-type determination conditions, Rayleigh scattering theory can be used to study the scattering effect of haze particles. The total scattering

TABLE 3. Particle scale distribution parameters of haze at different levels.

Case	PM2.5/μg · m^{-3}	r_g(μm)	σ_g(μm)	N_s(1/cm^3)
Slight haze	75	0.13	2.4	2700
Mild haze	103	0.15	2.39	3500
Moderate haze	145	0.16	2.41	4800
Severe haze	196	0.2	2.4	7000

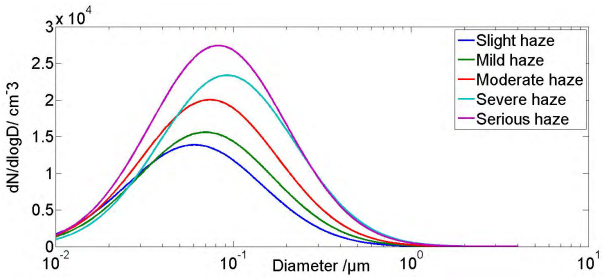

FIGURE 1. Haze particle distribution at different levels of pollution.

coefficient of terahertz waves caused by aerosol particles can be calculated based on the number density, haze particle scale distribution, and Rayleigh scattering cross-section.

B. PHYSICAL CHARACTERISTICS OF WATER DROPLETS

Moist water vapor condenses on haze particles and naturally absorbs moisture, enlarging the vapor and forming condensed nuclei. Fog is formed when the radius of the agglomerated core gradually increases to above 1μm. Fog occurs in the atmosphere close to the ground; it is a colloidal system composed of tiny water droplets or ice crystals that slowly settle in air near the ground, a product of water vapor condensation in the air. When a terahertz wave is transmitted in the fog, it interacts with droplet particles, resulting in signal attenuation. The typical diameter of a droplet is between a

TABLE 4. Relationship between visibility and meteorological state of fog.

Visibility class	0	1	2	3	4
Meteoro-logical state	Dense fog	Thick fog	Medium fog	Light fog	Mist
Visibility (km)	<0.05	0.05~0.2	0.2~0.5	0.5~1	1~2

few micrometers and several tens of micrometers. Because the droplet particle size is equal to the signal light wavelength, the impact of droplet particles on the transmitted signal mainly involves Mie scattering. The scope of visibility corresponding to different degrees of fog appears in Table 4.

The particle radius obeys a certain distribution, namely based on droplet size. The most commonly used reference is Deirmendiian droplet distribution, calculated by the following generalized Gamma distribution [20]:

$$n(r) = \mathrm{a} r^{\alpha} exp(-br^{\beta}) \tag{2}$$

Where r is the radius of a droplet particle, and n is the number of dropletswith radius of $r + dr$ in unit volume. If the radius of droplets is measured in micrometers (μm), then the unit of n is $\mathrm{m}^{-3}\mu m^{-1}$. The other parameters a and b that describe the droplet size and shape are determined by visibility and water content:

$$a = \frac{9.781}{V^6 M^5} \times 10^{15} \tag{3}$$

$$b = \frac{1.304}{VM} \times 10^4 \tag{4}$$

Where V is the visibility of fog (unit: km), and M is the water content of fog (unit: $\mathrm{g/m}^3$). The Gamma [21] droplet size distribution model applies when $\alpha = 2, \beta = 1$, which describes the size distribution of droplets:

$$n(r) = ar^2 exp(-br)(\mathrm{m}^{-4}) \tag{5}$$

According to the formation area and mechanism, fog can be divided into two categories: advection fog and radiation fog. Fog classification is mainly based on the sea surface and continental environment. Due to the large amount of water vapor on the sea, advection fog is most common on the sea surface; radiation fog is most common inland given a lack of water vapor. The relationship between the liquid water content M ($\mathrm{g/m}^3$) of fog and visibility V (km) can be expressed empirically.

$$\begin{cases} M = (18.35V)^{-1.43} = 0.0156V^{-1.43} & Advection\ fog \\ M = (42V)^{-1.54} = 0.00316V^{-1.54} & Radiation\ fog \end{cases} \tag{6}$$

Typical values can be used to represent liquid water density M. For medium fog, the liquid water density is often approximately $0.05\mathrm{g/m}^3$ (approximate visibility of 300m), where as that of dense fog is $0.5\mathrm{g/m}^3$(approximate visibility of 50m). Combining the above two formulas results in the following:

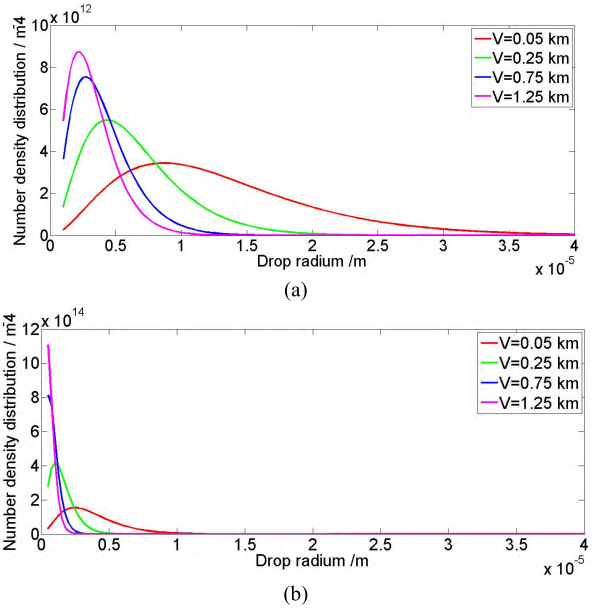

FIGURE 2. Droplet size distribution of advection fog and radiation fog under different degrees of visibility. (a) Advection fog. (b) Radiation fog.

1) Relationship between droplet distribution $n(r)$ and optical visibility V of advection fog:

The unit of r is m:

$$n(r) = 1.059 \cdot 10^{25} V^{1.15} r^2 exp\left(-8.359 \cdot 10^5 V^{0.43} r\right)(\mathrm{m}^{-4}) \tag{7}$$

The unit of r is μm:

$$n(r) = 1.059 \cdot 10^7 V^{1.15} r^2 \times exp\left(-0.8359 \cdot V^{0.43} r\right)\left(m^{-3}\mu m^{-1}\right) \tag{8}$$

2) Relationship between droplet distribution $n(r)$ and optical visibility V of radiation fog:

The unit of r is m:

$$n(r) = 3.104 \cdot 10^{28} V^{1.7} r^2 exp\left(-4.122 \cdot 10^6 V^{0.54} r\right)(\mathrm{m}^{-4}) \tag{9}$$

The unit of r is μm:

$$n(r) = 3.104 \cdot 10^{10} V^{1.7} r^2 \times exp\left(-4.122 \cdot V^{0.54} r\right)\left(\mathrm{m}^{-3}\mu\mathrm{m}^{-1}\right) \tag{10}$$

The droplet size distribution of advection fog and radiation fog under different degrees of visibility is shown in Fig. 2.

Small droplets dominate in fog with little visibility. As visibility increases, the content of small droplets gradually decreases, and the overall droplet size becomes larger. Therefore, small particles in fog have a greater impact on visibility than large particles. At the same time, the number of droplets in radiation fog is higher than in advection fog.

C. PHYSICAL CHARACTERISTICS OF RAINDROPS

Rainfall is a common phenomenon in nature. The diameter D of raindrops is between 100μm and 10mm. Generally, raindrops smaller than 5.5mm are called stable, whereas those larger than 5.5mm are unstable and prone to chipping or deformation, called temporary raindrops. Therefore, the raindrop radius is generally between 0.05mm and 4mm. The range of rainfall rate R corresponding to different types of rainfall is as follows: light rain(1mm/h); moderate rain(4 mm/h); heavy rain(16 mm/h); torrential rain (100 mm/h).The attenuation of terahertz signals caused by raindrops mainly depends on the raindrop size distribution, scattering, and absorption cross-section. Different raindrop distributions are used for different rainfall rates. The attenuation coefficient of terahertz signals caused by rain can be calculated using Mie scattering theory. The common raindrop spectrum distribution models include the Marshall-Palmer(M-P) distribution [22], Joss distribution [23], and Weibull distribution [24]. Due to a high level of accuracy and fitting degree, these three types of distributions are most commonly used by scholars and experts.

Based on the measured data of Laws and Parsons [25], Marshall and Palmer proposed a negative exponential distribution model, the M-P distribution, expressed as follows:

$$N(D) = 8000exp\left(-4.1\,R^{-0.21}D\right)(\mathrm{m}^{-3}\cdot\mathrm{mm}^{-1}), \quad D = 2r \tag{11}$$

Rainfall types are categorized as either drizzle, widespread, or thunder storm according to Joss and other researchers using the raindrop spectrometer, otherwise known as the Joss distribution. The size distribution of different types of raindrops represents a negative exponential distribution with different coefficients and the following expression:

$$\text{Drizzle}: N(D) = 30000exp(-5.7R^{-0.21}D) \tag{12}$$

$$\text{Widespread}: N(D) = 7000exp\left(-4.1R^{-0.21}D\right) \tag{13}$$

$$\text{Thunderstorm}: N(D) = 1400exp(-3.0R^{-0.21}D) \tag{14}$$

The Weibull raindrop distribution is derived strictly from the raindrop formation process, which can fully reflect the distribution of differently size raindrops. The expression of the Weibull distribution is as follows:

$$N(D) = N_0\frac{\eta}{\sigma}\left(\frac{D}{\sigma}\right)^{\eta-1}exp[-a\left(\frac{D}{\sigma}\right)^{\eta}] \tag{15}$$

A commonly used Weibull distribution parameter was proposed by Sekine: $N_0 = 1000$, $\eta = 0.95R^{0.14}$, $\sigma = 0.26R^{0.42}$, $a = 1$. Fig. 3 are raindrop size distributions of 2mm/h, 5 mm/h, 15mm/h, and 55 mm/h rainfall, respectively, corresponding to light rain, moderate rain, heavy rain, and rainstorm. The following four plots of Fig.3 show the comparison of three raindrop size distributions for four rainfall types.

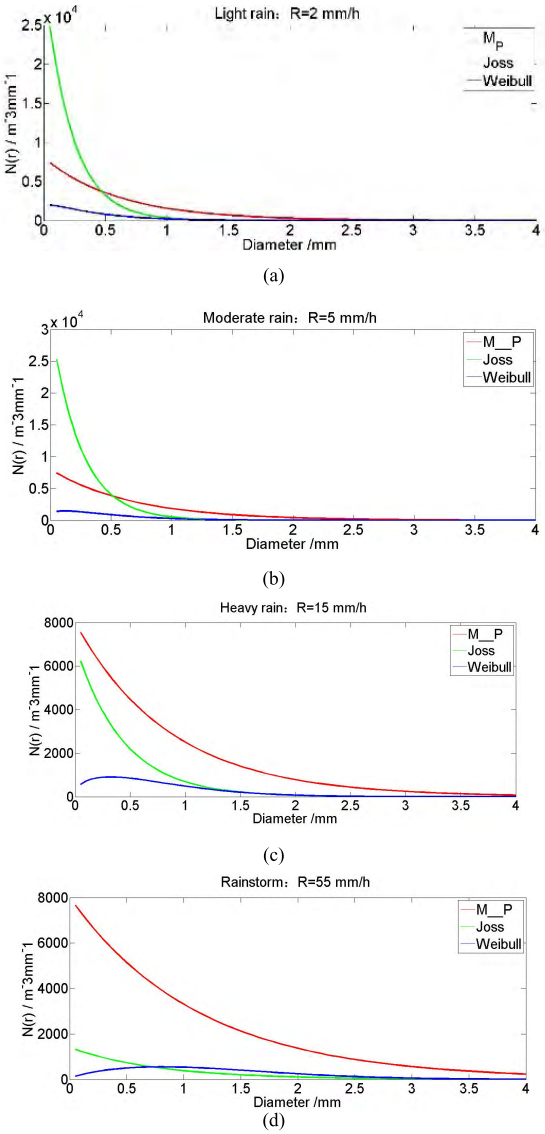

FIGURE 3. Comparison of three raindrop size distributions for four rainfall types. (a) Light rain. (b) Moderate rain. (c) Heavy rain. (d) Rainstorm.

Droplets with a diameter smaller than 1mm account for most droplets at different rainfall rates. With an increase in rainfall rate, the number of droplets with a diameter larger than 1 mm increases slightly. The M-P distribution and Weibull distribution are close when measuring light rain and moderate rain; in the case of heavy and rainstorm, the Joss distribution and Weibull distribution are close. Studies have shown that the attenuation calculated by the Weibull distribution is smaller than the given insufficient estimation of the number of small raindrops, while the Joss distribution's simulation of raindrops is more accurate under light, moderate, and heavy rain conditions in calculating rain attenuation more precisely. Therefore, this paper uses the Joss distribution spectrum to calculate the scattering attenuation effect of terahertz waves under different rainfall conditions. The Joss raindrops distribution of rainfall types is shown in Fig. 4.

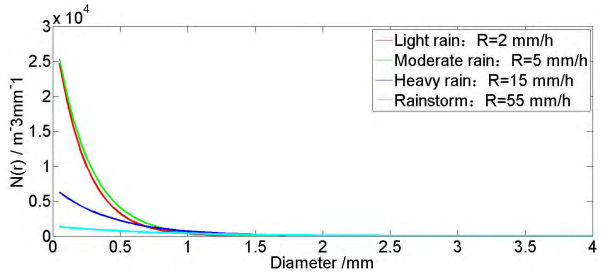

FIGURE 4. Joss raindrops distribution of rainfall types.

III. STUDY ON NEAR-SURFACE ATMOSPHERIC SCATTERING ATTENUATION OF TERAHERTZ WAVES

The attenuation of terahertz waves caused by fog, haze, and raindrops is considered in the near-surface atmosphere. The scattering effects of these three types of atmospheric particles on the wave can be analyzed by Rayleigh scattering and Mie scattering, respectively, according to different wavelength ranges and particle sizes. Determination of the scattering type posits that scattering formed by particles with a diameter larger than 0.03 times the wavelength is Mie scattering; otherwise, Rayleigh scattering occurs.

A. NUMERICAL CALCULATION METHOD OF PARTICLE SCATTERING ATTENUATION IN FOGGY WEATHER

Haze is a unique meteorological phenomenon with a complex composition. The particle number density distribution and characteristics of haze are often expressed by lognormal distributions. When calculating the radiation characteristics of haze particles, particles can be considered smooth, homogenous, non-magnetic circular particles for calculation convenience with no loss of rationality. For droplet particles and haze particles, the wavelength of the terahertz wave is in a critical application region of two-scattering theory; therefore, only one scattering theory can be used to calculate scattering attenuation. Particles with different scales in a given frequency range should be studied using the corresponding scattering theory.

Rayleigh scattering occurs when the scattering particle size is much smaller than the wavelength. As shown in the statistical Table 2, 3 and 4 of particle density of haze and fog, most particle diameters are concentrated in the range of 0.01–1μm. Therefore, the haze particle radius is much smaller than the terahertz wavelength, leading to primarily Rayleigh scattering. Scattering coefficients are used to describe signal attenuation due to particle scattering. Therefore, the scattering attenuation of the line-of- sight signal can be modeled using the inverse Beer-Lambert law. The definitions of transmittance and absorption are similar, and the total attenuation of scattering is defined as

$$A_{sca}(f) = \exp\left(\sum_j k_s^j(f)\, r\right) \tag{16}$$

The scattering effect caused by different scales of particles can be summed, and the scattering coefficient of scattering particles j is

$$k_s^j(f) = N_s^j \sigma_s^j(f) \tag{17}$$

Where N_s^j is the number density of scattering particles $j \cdot \sigma_s^j(f)$ is the scattering cross-section of particles j, which is a function of the frequency f of the transmission signal. Different types of particles j have different radii. Rayleigh scattering properties are given by the Rayleigh scattering cross-section. Various methods can be used to evaluate the scattering cross-section. First, the Rayleigh scattering cross-section of a classical hard spherical scatterer can be calculated by the following formula [26]:

$$\sigma_s(f) = \frac{128\pi^5\beta^2}{3\lambda^4} \tag{18}$$

Where λ is the wavelength corresponding to the frequency f of the terahertz signal, and β is the polarizability of the molecule, approximated as [27]

$$\beta = \frac{m(f)^2 - 1}{m(f)^2 + 2}\left(\frac{d}{2}\right)^3 \tag{19}$$

Where $m(f)$ is the refractive index of the medium at the frequency f, and the diameter of the aerosol is d. In the absence of refractive index measurement data in the terahertz band, approximately $m(f) = 1.6$ [28] is considered at all frequencies, representing the approximate average refractive index of mineral dust at visible frequencies. As such, the hard sphere scattering cross-section depending on particle diameter is as follows:

$$\sigma_s(f) = \frac{2\pi^5 d^6}{3\lambda^4}\left(\frac{m(f)^2 - 1}{m(f)^2 + 2}\right)^2 \tag{20}$$

Fig. 5 shows the scattering cross-section of different-diameter particles in the terahertz band compared to frequency. The higher the frequency, the stronger the scattering effect.

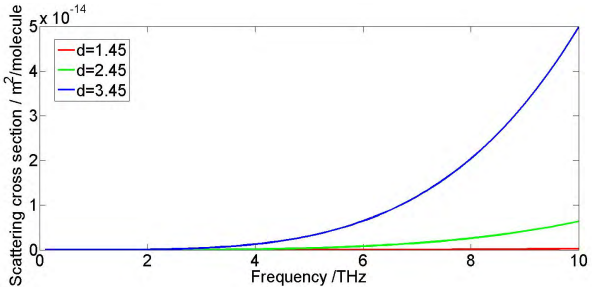

FIGURE 5. Scattering cross-section of different diameter particles in the terahertz band vs. frequency.

Assuming aerosol scattering is elastic (i.e., the wavelength of the electromagnetic wave does not change due to scattering events), Eq. (20) can be used to analyze particle scattering. This article also assumes that aerosol particles are perfect scatterers (i.e., the imaginary part of the refractive index is zero, such that the absorption coefficient of aerosol particles

is zero). To calculate the total scattering coefficient of aerosol particles, Eq. (1) must be multiplied by the number density N_s and the scattering cross-section of Eq. (20) and then integrated on the radius of all particles to obtain the aerosol scattering coefficient.

$$k_s^j(f) = \int_0^\infty \sigma_s(f) \cdot N(d) * N_s dd \tag{21}$$

Unit: cm^2/molecular, where superscript j refers to different particle types.

Rayleigh scattering theory was used to calculate the scattering attenuation of the terahertz wave caused by haze particles. Due to an absence of measurement data, the refractive index of haze particles was assumed to be the average aerosol refractive index of m= 1.6. ThecharacteristicRayleigh scattering attenuation of the terahertz wave caused by different levels of haze compared to frequency is shown in Fig. 6. The haze scattering attenuation at the lower frequency band was quite small, but as the frequency increased, attenuation became increasingly strong. The more severe the pollution, the more pronounced the scattering attenuation of the terahertz wave caused by the haze particles. Fig. 6 also illustrates that when the frequency was10 THz, the haze particle characteristic attenuation in severely hazy conditionswas0.75 dB higher than in a slight haze.

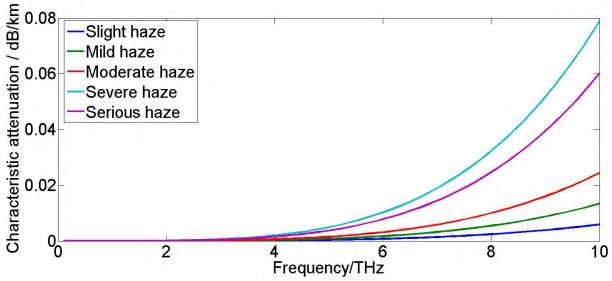

FIGURE 6. Characteristic scattering attenuation caused by different levels of haze vs. frequency.

Because the concentration of pollutant gases such as O_3, CO, NO_2, and SO_2 exceeds standard values under hazy conditions, the absorption and attenuation of terahertz waves by these pollutant gases cannot be ignored. Typical pollutant gas concentrations were determined according to data on six pollutant concentrations in cities in China. The absorption attenuation of terahertz waves caused by O_3, CO, NO_2, and SO_2 was calculated using the line-by-line integration method. Taking CO as an example, the absorption characteristic attenuation of a terahertz wave caused by CO is shown in Fig. 7.

The absorption attenuation of a terahertz wave caused by CO wasrelatively strong in the frequency band between 0.1–3.5 THz. The absorption attenuation peaks and valleys outside this band essentially did not exist; that is, the frequency selection characteristics basically disappeared. The characteristic absorption attenuation of terahertz waves caused by O_3, NO_2, and SO_2 was calculated similarly and

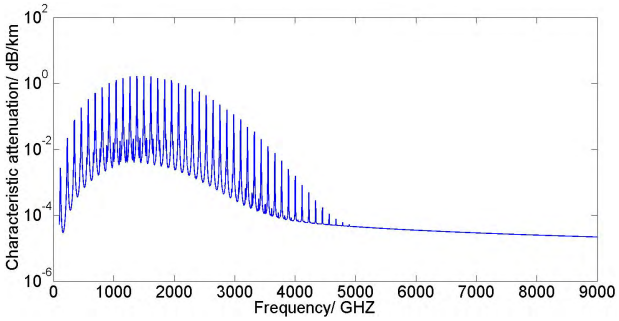

FIGURE 7. Absorption characteristic attenuation of terahertz wave caused by CO.

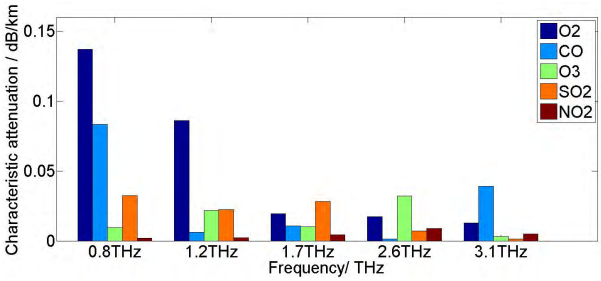

FIGURE 8. Absorption attenuation of terahertz waves by various pollutant gases at different frequencies.

compared to the characteristic attenuation value of five frequency points at 0.8THz, 1.2THz, 1.7THz, 2.6THz, and 3.1THz, respectively as Fig. 8.

The absorption attenuation of terahertz waves caused by pollutant gases exhibited strong frequency selectivity, and the absorption effects of terahertz waves caused by the same gases differed at specific frequencies. Again taking CO as an example, the characteristic attenuation of the 0.8 THz wave was0.077 dB higher than the 0.12 THz wave. The absorption effects caused by different gases were also unique; the characteristic attenuation of the 0.8THz wave caused by CO was0.074 dB higher than that caused by O_3. When the frequency was below 4.2 THz, the absorption peaks of O_3 weredense. The higher the frequency, the sparser the absorption peaks and valleys. Obvious absorption peaks appeared at 0.84 THz, 1.58 THz, 2.3 THz, and 2.65 THz. The absorption effect of NO_2 was also concentrated in the lower frequency band. When the frequency exceeded 2.2THZ, the absorption attenuation could be neglected. An increase in frequency led to sparser peaks and valleys of the absorption attenuation curve for SO_2, and the absorption intensity declined. When the frequency was above 7.98 THz, the absorption attenuation was negligible. For these four types of gases, absorption attenuation intensity tended to decrease and frequency selectivity became weaker with increasing frequency.

B. NUMERICAL METHOD OF PARTICLE ATTENUATION IN FOG

1) RAYLEIGH APPROXIMATING SMALL DROPLET SCATTERING ATTENUATION METHOD

The Rayleigh approximation condition is calculated as $|n| \cdot \chi < 0.5$, where n is the complex index of refraction of the

scattering particles [29] and χ is a dimensionless size parameter, $\chi = 2\pi r/\lambda$, determined by the signal wavelength λ and the particle radius r. Scattering attenuation caused by the particle group satisfying this condition can be calculated using the Rayleigh approximation method. The frequency range of different particle radii satisfying this approximate calculation condition also varies, although the Rayleigh approximation method can only be used within a certain frequency range. For small droplets with radii of 0.01–10 microns, when the terahertz frequency spans 0.01–1 THz, the dimensionless size parameter satisfies the Rayleigh scattering condition. The droplet also consists of water, which simplifies the calculation process. The Rayleigh approximation method can be used to calculate the attenuation of terahertz waves by small droplets; the electromagnetic transmission characteristics of water droplets depend on the size distribution, particle shape, dielectric constant, and other factors.

When Rayleigh approximation conditions are satisfied, the extinction coefficient scattering term can be ignored, leaving only the absorption term. Therefore, it is unnecessary to accurately calculate the droplet density distribution. According to Rayleigh approximation, the attenuation of the terahertz wave caused by smaller droplets within fog can be calculated as:

$$\alpha_c = K_f \cdot M \mathrm{dB/km} \tag{22}$$

Where M is liquid water density in fog$(\mathrm{g/m^3})$.K_f is the specific attenuation coefficient measured as $(\mathrm{dB/km})/(\mathrm{g/m^3})$, calculated as:

$$K_f = \frac{0.819f}{\varepsilon''(1+\eta^2)} \tag{23}$$

$$\eta = \frac{2+\varepsilon'}{\varepsilon''} \tag{24}$$

Where f is the signal frequency(GHz), and ε' and ε'' are the real and imaginary parts of the complex dielectric permittivity of water, respectively. The complex permittivity of water can be obtained using the double Debye model [30], in which the complex refractive index of water droplets is calculated as

$$m = \sqrt{\frac{\sqrt{\varepsilon'^2 + \varepsilon''^2} + \varepsilon'}{2}} \tag{25}$$

Fig.9 shows the value of K_f at frequencies from 10–1000 GHz and different temperatures. K_f increased as the temperature declined and the frequency was low; K_f was higher when the temperature rose and the frequency was high.

The association between water content and visibility in fog can be obtained by Eq. (6). When visibility was fixed, the characteristic attenuation of terahertz waves caused by droplets decreased with increasing temperature at lower frequency bands and increased with temperature at higher frequency bands. Characteristic attenuation increased as the frequency climbed. The effect of temperature on attenuation was not found to be significant at low-frequency bands but was significant at high-frequency bands as shown in Fig. 10.

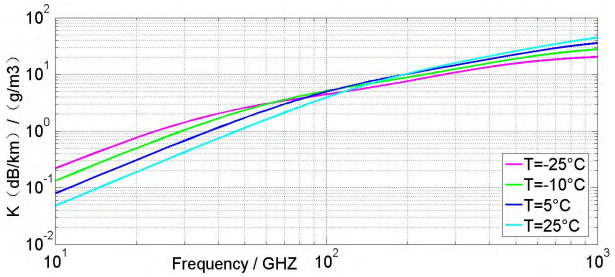

FIGURE 9. Specific attenuation coefficient of water droplets at various temperatures as a function of frequency.

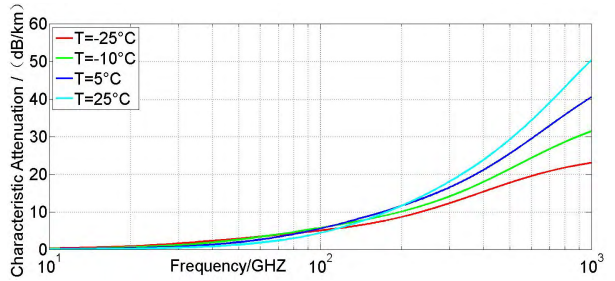

FIGURE 10. Characteristic attenuation at various temperatures as a function of frequency.

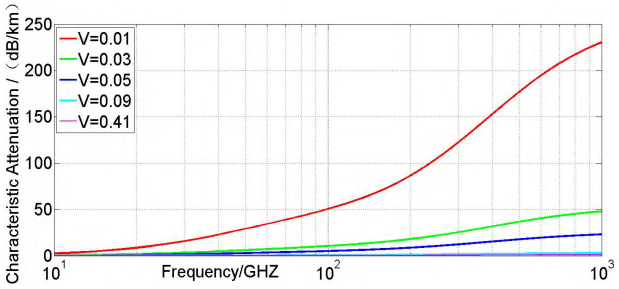

FIGURE 11. Characteristic attenuation at various visibility as a function of frequency.

The water content in fog varies at different fog intensities and directly affects visibility. The higher the water content, the lower the visibility, and the more significant the attenuation effect on the terahertz wave. Fig. 11demonstrates that as the visibility decreased, the amplitude of characteristic attenuation increased exponentially. When the visibility decreased from 0.05km to 0.03km at a frequency of 1THz, the characteristic attenuation per kilometer increased by 25dB; when the visibility decreased from 0.03km to 0.01km, the characteristic attenuation increased by 182 dB, and the characteristic attenuation increased by nearly 8 times due to the exponential relationship between water content M and visibility V.

2) THE CALCULATION OF SCATTERING ATTENUATION OF FOG DROPLETS BY MIE THEORY

As the particle size gradually increases to be comparable with the wavelength, Rayleigh scattering fails, and Mie scattering

occurs instead. The scattering effect is generally considered to be Mie scattering either when the particle parameter satisfies the condition of $\chi = 2\pi r/\lambda > 0.1$–$0.3$ or when the diameter is greater than the wavelength of 0.03 times. In a typical fog, the size of large droplets with radii in the range of 20–60μm is comparable to the wavelength of the signal in the terahertz band range. Therefore, the effects of droplet particles on the transmitted signal is mainly Mie scattering.

Mie scattering theory was proposed by Mie in 1908 and proposes a scattering rule for uniform spherical particles with a certain range of diameters and arbitrary components; this method systematically expounds the scattering mechanism of electromagnetic waves using particles of various sizes in the atmosphere. The extinction characteristics of aerosols are determined by parameters such as the average radius, signal frequency, complex refractive index, and particle size distribution. The scattering characteristics of a terahertz wave transmitted in the atmosphere can be described by the absorption factor, absorption coefficient, scattering factor, scattering coefficient, extinction factor, and extinction coefficient. The radiation properties of individual particles can be described by absorption factors, scattering factors, and extinction factors. The absorption coefficient, scattering coefficient, and extinction coefficient indicate the radiation properties of the whole particle system. According to this theory, the scattering coefficient is related to the wavelength λ, particle radius r, and complex refractive index m and can be calculated as follows:

$$a_n = \frac{\psi_n(x)\,\psi_n'(mx) - m\psi_n'(x)\,\psi_n(mx)}{\zeta_n(x)\,\psi_n(mx) - m\zeta_n(x)\,\psi_n(mx)} \tag{26}$$

$$b_n = \frac{m\psi_n(x)\,\psi_n'(mx) - \psi_n'(x)\,\psi_n(mx)}{m\zeta_n(x)\,\psi_n(mx) - \zeta_n(x)\,\psi_n(mx)} \tag{27}$$

Where $\psi_n(x)$ and $\zeta_n(x)$ are the first and third types of Bessel functions, respectively, and x is a dimensionless size parameter where $x = kr$, $k = 2\pi/\lambda$. Signal attenuation by particles is mainly reflected in absorption and scattering effects. When using Mie scattering theory to study the scattering attenuation characteristics of signals, it is necessary to focus on three main parameters: the absorption efficiency factor $Q_a(x, m)$, scattering efficiency factor $Q_s(x, m)$, and extinction efficiency factor $Q_e(x, m)$.

$$Q_e(x, m) = \frac{2}{x^2}\sum_{n=1}^{\infty}(2n+1)Re(a_n + b_n) \tag{28}$$

$$Q_s(x, m) = \frac{2}{x^2}\sum_{n=1}^{\infty}(2n+1)\{|a_n|^2 + |b_n|^2\} \tag{29}$$

$$\mathrm{Q_a(r, \lambda, m) = Q_e(r, \lambda, m) - Q_s(r, \lambda, m)} \tag{30}$$

Fig.12 depicts the relationship between scattering efficiency factor Q_e and dimensionless size parameter x. The scattering efficiency factor oscillated up and down with an increase of the dimensionless size parameter until finally plateauing to $Q_e = 2$.

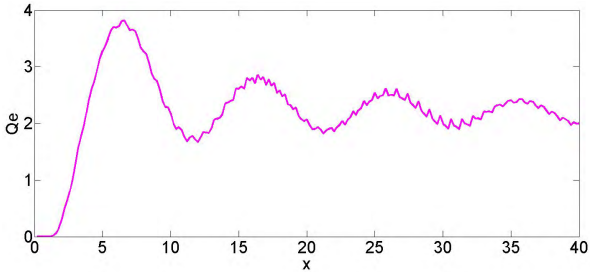

FIGURE 12. Relationship between scattering efficiency factor Q_e and size parameter x.

The scattering cross-section $\delta_s(\mathrm{r}, \lambda, m)$ is defined thusly: the incident wave acts on a cross-section with an area such that the power of the incident wave in this section is equal to the sum of the scattered power of the particles in all directions. Similarly, the following relationship exists between the absorption cross-section $\delta_a(\mathrm{r}, \lambda, m)$ and the extinction section $\delta_e(\mathrm{r}, \lambda, m)$:

$$\delta_e(\mathrm{r}, \lambda, m) = \delta_s(\mathrm{r}, \lambda, m) + \delta_a(\mathrm{r}, \lambda, m) \tag{31}$$

Dividing the total scattering cross-section by πr^2 yields the normalized scattering cross-section (i.e., the scattering efficiency factor). The absorption cross-section and extinction cross-section are the same; therefore, the relationship between the cross-section and corresponding efficiency factor is as follows:

$$\delta(\mathrm{r}, \lambda, \mathrm{m}) = \pi \mathrm{r}^2 \mathrm{Q}(\mathrm{x}, \mathrm{m}) \tag{32}$$

The expression of the scattering section and extinction section is thus

$$\delta_e(\mathrm{r}, \lambda, \mathrm{m}) = \frac{\lambda^2}{2\pi}\sum_{n=1}^{\infty}(2\mathrm{n}+1)\mathrm{Re}(\mathrm{a_n} + \mathrm{b_n}) \tag{33}$$

$$\delta_s(\mathrm{r}, \lambda, \mathrm{m}) = \frac{\lambda^2}{2\pi}\sum_{n=1}^{\infty}(2\mathrm{n}+1)\{|\mathrm{a_n}|^2 + |\mathrm{b_n}|^2\} \tag{34}$$

The relationship between the dimensionless size parameter and the scattering cross-section is

Regardless of the refractive index, when x is small, Q_s is much less than 1, and the particle scattering energy is hence much smaller than the energy projected on its geometric section. As x increases, Q_s also increases rapidly and then decays to 2 in the form of damped oscillations. As the refractive index increases, the maximum value of Q_s also increases slightly

For haze particles with a given size distribution $n(r)$, the signal attenuation of the unit distance (i.e., characteristic attenuation) is

$$\mathrm{A} = 4.343 \cdot 10^3 \int_0^{\infty} \mathrm{Q_e(r)\,n(r)\,dr} \quad (\mathrm{dB/km}) \tag{35}$$

Droplets can be assumed to be composed completely of water molecules; therefore, the water content can be used to describe droplet characteristics. First, Eq.(28) is used to calculate the scattering efficiency factor Q_e of different radius droplets for the terahertz wave. The relationship between

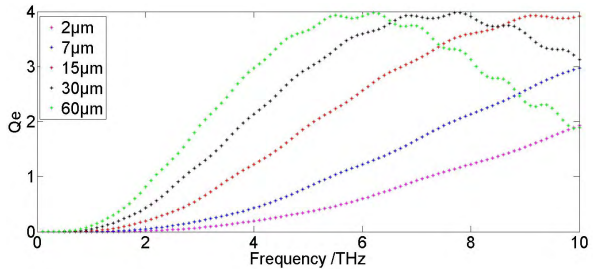

FIGURE 13. Attenuation efficiency factor for droplets of different sizes vs. frequency. (a) Advection fog. (b) Radiation fog.

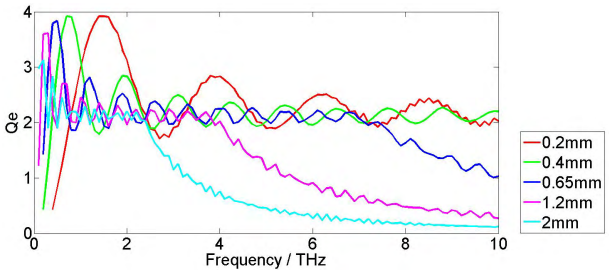

FIGURE 15. Scattering efficiency factor for different size of raindrops as a function of frequency.

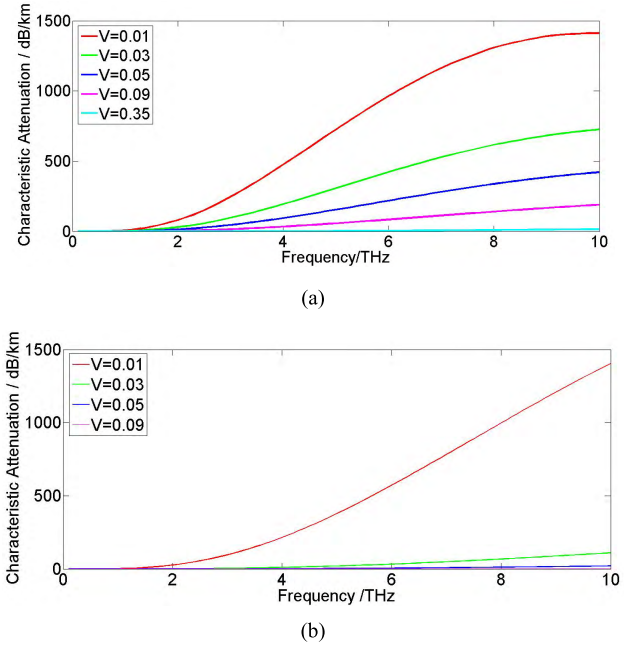

FIGURE 14. Characteristic attenuation of terahertz wave at a frequency band of 0.1–10THzunderdifferent visibilities.

the scattering efficiency factor (i.e., extrinsic factor) and frequency f is shown in Fig. 13:

Fog droplets obey the Gamma distribution; the attenuation coefficient of the particle system can be obtained by combining the scattering cross-section of the individual particles and the overall distribution spectrum of droplets, which are then integrated on the particle radius. Fig.14 shows the characteristic attenuation of the terahertz wave at a frequency band of 0.1–10THz at different degrees of visibility for advection fog and radiation fog, respectively.

As the frequency increased, so did the scattering attenuation of the terahertz wave by fog droplets, which demonstrates a trend of an increase at the lower band and a decrease at the higher band. The scattering attenuation by fog droplets also increased exponentially with a decrease invisibility for two kinds of fog. The characteristic attenuation of advection fog was 426 dB, 728 dB, and 1407 dB at a visibility of 0.05 km, 0.03 km, and 0.01 km, respectively, at a frequency of 10THz.The characteristic attenuation was 50 dB, 165 dB, and 1483 dB, respectively, for radiation fog. The increasing rate of the characteristic attenuation intensity of radiation fog was significantly greater than that of advection fog because the effect of water content on visibility varied for different types of fog. Visibility also affected droplet size distribution, thus affecting attenuation intensity.

C. CALCULATION OF SCATTERING ATTENUATION OF RAINDROPS USING MIE THEORY

For steady-state raindrop particles, the radii are generally considered to be between 0.05mm–4mm; therefore, Mie scattering is dominant. The refractive index of raindrop particles at different frequencies can be calculated using the double Debye model. The size distribution of raindrops is related to rainfall type: meteorological rainfall intensity is divided into light rain (0–2.5mm/h), moderate rain (2.6–8mm/h), heavy rain (8.1–15.9mm/h), and rainstorm (more than 16 mm/h). Rain drop distribution can be described at different rainfall rates using the Joss distribution. The Mie scattering method can be used to study the attenuation of terahertz waves under different raindrop sizes. The scattering efficiency factor for different sizes of raindrops is shown in Fig. 15 as a function of frequency.

The scattering efficiency factor for small raindrops fluctuated around $Q_e = 2$ eventually plateauing to 2. The scattering efficiency factor for large raindrops is approximate to 2 in the low-frequency range and decreased sharply as the frequency increased, rendering the approximation no longer applicable. Rainfall rates were2mm/h, 5mm/h, 15mm/h, 55mm/h, and 95mm/h, respectively, corresponding to light rain, moderate rain, heavy rain, and rainstorm. Fig. 16 shows the raindrop distribution under different rainfall rates. Raindrops were mainly concentrated in a small size range under rainy conditions. As the rate of rainfall increased, the number of small raindrops declined sharply, while the number of large raindrops increased.

Fig.17 shows the characteristic attenuation of terahertz waves under different rainfall types as a function of frequency. In the low-frequency range, the attenuation effect of rainfall on the terahertz waves increased in line with the rainfall rate; that is, the scattering effect of large raindrops on terahertz waves was stronger than that of small raindrops in the low-frequency range. The strongest scattering attenuation

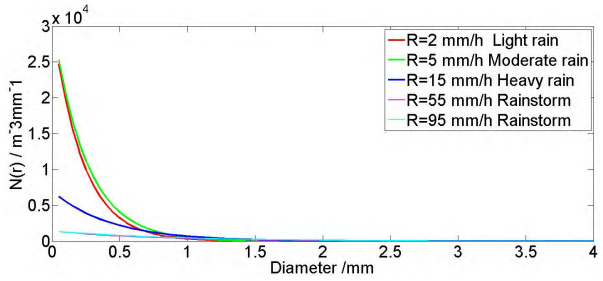

FIGURE 16. Raindrop distributions under different rainfall rates.

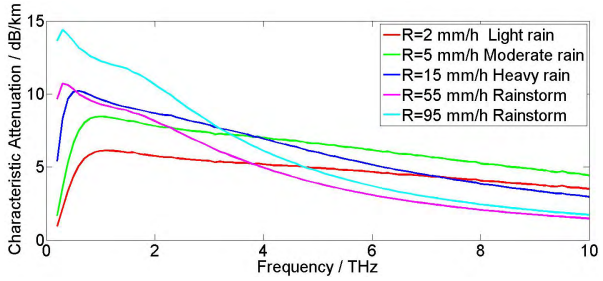

FIGURE 17. Characteristic attenuation under different rainfall rates as a function of frequency.

position was in the vicinity of 1.15 THz for moderate and light rain, 0.6 THz for heavy rain, and 0.3 THz for rainstorm. As the rate of rainfall increased, the extreme point of characteristic attenuation moved to the low-frequency band. However, as the frequency increased, the attenuation effect of rainfall on the terahertz wave gradually decreased with an increase in the rainfall rate; the effect of raindrop size on the scattering effect decreased in the high-terahertz band, and the number of small particles was much greater than that of large particles.

IV. CONCLUSION

In this paper, the scattering attenuation of terahertz waves by atmospheric particles is studied based on Mie and Rayleigh scattering theory. The diameter, number density, complex refractive index, size distribution, and other optical characteristic parameters of particles were obtained from meteorological data and the literature. The characteristic attenuation of terahertz waves under different particle types and sizes was calculated using Mie scattering theory and Rayleigh scattering theory, respectively. We obtained the following conclusions.

1. The scattering effect of haze particles on terahertz waves increased with frequency and pollution level. The characteristic attenuation of serious haze was 0.75 dB higher than that of slight haze at a frequency of 10THz. The absorption peaks were high in frequency bands below 4.2 THz for O_3. Absorption attenuation caused by NO_2 was also concentrated in the low-frequency band, which can be ignored at frequency bands above 2.2THz. The peaks and troughs of the characteristic absorption attenuation curve of SO_2 became increasingly sparse, and the absorption intensity decreased with frequency. When the frequency was above 7.98 THz, absorption attenuation could be ignored. Absorption attenuation intensity tended to decrease, and frequency selectivity became weaker with increasing frequency for four types of gas as CO, O_3, SO_2 and NO_2.
2. The water content in the fog was negatively correlated with visibility. The greater the water content, the more significant the attenuation effect of the terahertz wave. The characteristic attenuation amplitude increased exponentially as visibility decreased. At visibilities of 0.05 km, 0.03 km, and 0.01 km at a frequency of 1 THz, the scattering characteristics per kilometer were 23 dB, 47.8 dB, and 230.4 dB, respectively.
3. The scattering attenuation of terahertz waves caused by large droplets increased exponentially with a decreasing in visibility for advection fog and radiation fog. The attenuation characteristics of advection fog were 426 dB, 728dB, and 1407dB, respectively, at visibilities of 0.05km, 0.03km, and 0.01km with frequency of 10THz, which were 50 dB, 165dB, and 1483 dB, respectively for radiation fog at the same visibilities. The increasing rate of attenuation intensity for radiation fog was significantly greater than that of advection fog, because the effect of water content on visibility varied for different fog types, thus affecting attenuation intensity.
4. When the rainfall rate increased, the number of small raindrops decreased drastically, and the number of large raindrops increased. As a result, in the low-frequency range, the attenuation effect of rainfall on the terahertz wave increased with the rainfall rate. This phenomenon suggested that large raindrops scattered terahertz waves more effectively than small raindrops in the low-frequency THz band. The strongest scattering attenuation was around 1.15 THz for medium and light rain. When the rainfall rate increased from 2 mm/h (light rain) to 5 mm/h (moderate rain), the characteristic attenuation increased from 6.1 dB to 8.4dB. As the rainfall rate continued to increase, the extreme points of characteristic attenuation moved towards the direction of the low-frequency band. The extreme point of characteristic attenuation was at 10.3 dB in heavy rain at a rainfall rate of 15 mm/h, near 0.6 THz. But the extreme point during rainstorm was near 0.3 THz. When the rainfall rate increases from 55 mm/h to 95 mm/h, the characteristic attenuation changes from 10.7 dB to 14.4dB. However, as the frequency increased, the attenuation effect of rainfall on the terahertz wave gradually decreased with an increase of the rainfall rate. The effect of particle size on scattering decreased in the high-frequency band.

As the measured attenuation data of terahertz waves in different meteorological environments increases, the existing channel model can be better modified, and the attenuation of

terahertz waves under more complex meteorological conditions such as atmospheric turbulence will be further studied.

REFERENCES

[1] I. F. Akyildiz, J. M. Jornet, and C. Han, "Terahertz band: Next frontier for wireless communications," *Phys. Commun.*, vol. 9, no. 1, pp. 16–32, 2014.
[2] J. M. Jornet and I. F. Akyildiz, "Channel modeling and capacity analysis for electromagnetic wireless nanonetworks in the terahertz band," *IEEE Trans. Wireless Commun.*, vol. 10, no. 10, pp. 3211–3221, Oct. 2011.
[3] M. L. Laucks, "Aerosol technology properties, behavior, and measurement of airborne particles," *J. Aerosol. Sci.*, vol. 31, no. 9, pp. 1121–1122, 1999.
[4] A. Ishimaru and S. T. Hong, "Multiple scattering effects on coherent bandwidth and pulse distortion of a wave propagating in a random distribution of particles," *Radio Sci.*, vol. 10, no. 6, pp. 637–644, Jun. 1975.
[5] H. Dougherty and E. Dutton, "Estimating year-to-year variability of rainfall for microwave applications," *IEEE Trans. Commun.*, vol. COM-26, no. 8, pp. 1321–1324, Aug. 1978.
[6] H. J. Liebe, "MPM—An atmospheric millimeter-wave propagation model," *Int. J. Infr. Millim. Waves*, vol. 10, no. 6, pp. 631–650, 1989.
[7] H. Vasseur and C. J. Gibbins, "Prediction of apparent extinction for optical transmission through rain," *Appl. Opt.*, vol. 35, no. 36, pp. 7144–7150, 1996.
[8] S. Lakshmi, Y. H. Lee, and J. T. Ong, "The role of particular rain drop size on rain attenuation at 11 GHz," in *Proc. 6th Int. Conf. Inf., Commun. Signal Process.*, Dec. 2007, pp. 1–4.
[9] D. R. Johnston and D. E. Burch, "Attenuation by artificial fogs in the visible, near infrared, and far infrared," *Appl. Opt.*, vol. 6, no. 9, pp. 1497–1501, Sep. 1967.
[10] J. Kokkoniemi, J. Lehtomäki, K. Umebayashi, and M. Juntti, "Frequency and time domain channel models for nanonetworks in terahertz band," *IEEE Trans. Antennas Propag.*, vol. 63, no. 2, pp. 678–691, Feb. 2015.
[11] B. A. Bodhaine, N. B. Wood, E. G. Dutton, and J. R. Slusser, "On Rayleigh optical depth calculations," *J. Atmos. Ocean. Technol.*, vol. 16, no. 11, pp. 1854–1861, 1999.
[12] J. G. Calvert, "Glossary of atmospheric chemistry terms," *Pure Appl. Chem.*, vol. 62, no. 11, pp. 2167–2219, 1990.
[13] I. F. Akyildiz and J. M. Jornet, "Electromagnetic wireless nanosensor networks," *Nano Commun. Netw.*, vol. 1, no. 1, pp. 3–19, Mar. 2010.
[14] Z. W. Zhao and Z. S. Wu, "Study on radio wave propagation characteristics and remote sensing of hydrometeors," (in Chinese), Ph.D. dissertation, Xidian Univ., Xi'an, China, 2001, pp. 78–82.
[15] J.-Q. Yao *et al.*, "Study and outlook of THz radiation atmospheric propagation," (in Chinese), *J. Optoelectron. Laser*, vol. 21, no. 10, pp. 1582–1588, 2010.
[16] S. G. Huang and M. Zhang, "Study on the transmission characteristic of terahertz wave," (in Chinese), Ph.D. dissertation, Xidian Univ., Xi'an, China, 2010, pp. 30–32.
[17] *Propagation Data Required for the Design of Terrestrial Free-Space Optical Links, (ITU-R) Standard*, document Rec. ITU-R, 2012, P. 1817-1.
[18] C. Zender. (2010). *Particle Size Distributions: Theory and Application to Aerosols, Clouds, Soils*. [Online]. Available: http://dust.ess.uci.Edu/facts/psd
[19] T. Hussein *et al.*, "Urban aerosol number size distributions," *Atmos. Chem. Phys.*, vol. 3, no. 5, pp. 391–411, 2003.
[20] X.-Z. Ke, D.-D. Ma, and J.-N. Liu, "Study attenuation of laser transmission in fog," *J. Light Scattering*, vol. 21, no. 2, pp. 104–109, 2009.
[21] J. F. Federici, L. Moeller, and K. Su, "Terahertz wireless communication," in *Handbook of Terahertz Technology for Imaging, Sensing and Communications* (Woodhead Publishing Series in Electronic and Optical Materials). Great Britain, 2013, pp. 156–214.
[22] S. Chandrasekhar, *Raiative Heat Transfer*. New York, NY, USA: Dover, 1960, pp. 237–266.
[23] J. S. Marshall and W. Palmer, "The distribution of raindrops with size," *J. Meteorol.*, vol. 5, pp. 165–166, Aug. 1948.
[24] J. Joss and E. G. Gori, "Shapes of raindrop size distributions," *J. Appl. Meteorol.*, vol. 17, no. 17, pp. 1054–1061, 1978.
[25] S. Assuline and Y. Mualem, "The similarity of regional rainfall: A dimensionless model of drop size distribution," *Trans. ASAE*, vol. 32, no. 4, pp. 1216–1222, 1989.
[26] J. O. Laws and D. A. Parsons, "The relationship of raindrop size to intensity," *Trans. Amer. Geophys. Union*, vol. 24, no. 2, pp. 248–262, 1943.
[27] D. Haubrich, J. Musser, and E. S. Fry, "Instrumentation to measure the backscattering coefficient b_b for arbitrary phase functions," *Appl. Opt.*, vol. 50, no. 21, pp. 4134–4147, 2011.
[28] K. Kandler *et al.*, "Chemical composition and complex refractive index of Saharan Mineral Dust at Izaña, Tenerife (Spain) derived by electron microscopy," *Atmos. Environ.*, vol. 41, no. 37, pp. 8058–8074, Dec. 2007.
[29] H. J. Liebe, G. A. Hufford, and T. Manabe, "A model for the complex permittivity of water at frequencies below 1 THz," *Int. J. Infr. Millim. Waves*, vol. 12, no. 7, pp. 659–675, 1991.
[30] H. Liebe, T. Manabe, and G. Hufford, "Complex permittivity of water between 0 and 30 THz," *Int. J. Infr. Milli.*, vol. 12, no. 7, pp. 677–682, 1991.

QINGFENG JING was born in 1981. He received the B.S., master's, and Ph.D. degrees from the School of Electronics and Information Engineering, Harbin Institute of Technology, in 2003, 2005, and 2009, respectively.

He has been an Associate Professor with the College of Astronautics, Nanjing University of Aeronautics and Astronautics, since 2009. He is currently in charge of several fund projects. His research interests are digital signal processing, satellite communication, terahertz communication, and wideband multi-carrier communication.

DANMEI LIU was born in 1995. She received the B.S. degree from the College of Astronautics, Nanjing University of Aeronautics and Astronautics, in 2016.

She is currently pursuing the master's degree with the College of Astronautics, Nanjing University of Aeronautics and Astronautics. Her research interests are satellite communication and terahertz communication.

JINCHENG TONG was born in 1979. He received the B.S. degree from the School of Electronics and Information Engineering, Harbin Institute of Technology, in 2003, and the master's degree in aircraft design from the China Academy of Space Technology in 2006.

He has been a Senior Engineer since 2014. His research interest is communication satellite design.